RGD constructs with physical anchor groups as polymer co-electrospinnable cell adhesives†

Paul J. Hommes-Schattmann[a], Axel T. Neffe[a,b], Bilal Ahmad[c], Gareth R. Williams[c], Gael M'Bele[d,e], Valérie Vanneaux[d,e], Philippe Menasché[f], David Kalfa[g], and Andreas Lendlein[a,b,*]

†: This article is published in Journal of Polymers for Advanced Technologies in the special issue on Advanced Functional Polymers for Medicine 2016, edited by Andreas Lendlein and Dirk W. Grijpma: Polym. Adv. Technol. 2017, 28 1312–1317.

a: Institute of Biomaterial Science and Berlin-Brandenburg Centre for Regenerative Therapies, Helmholtz-Zentrum Geesthacht, Teltow, Germany.

b: Institute of Chemistry, University of Potsdam, Potsdam, Germany.

c: UCL School of Pharmacy, 29-39 Brunswick Square, London, WC1N 1AX, UK.

d: Assistance Publique – Hôpitaux de Paris, Unité de thérapie cellulaire et CIC de Biothérapies, Hôpital Saint Louis, France.

e: UMR1160, Institut Universitaire d'Hématologie, 75475, Paris Cedex 10, France.

f: Department of Cardiovascular Surgery and INSERM U 970, Hôpital Européen Georges Pompidou; University Paris Descartes, Sorbonne Paris Cité Paris, France.

g: TEH Tube consortium coordinator, New York, NY, USA.

Correspondence to: A. Lendlein, E-mail: andreas.lendlein@hzg.de

Abstract:

The tissue integration of synthetic polymers can be promoted by displaying RGD peptides at the biointerface with the objective of enhancing colonization of the material by endogenous

cells. A firm but flexible attachment of the peptide to the polymer matrix, still allowing interaction with receptors, is therefore of interest. Here, the covalent coupling of flexible physical anchor groups, allowing for temporary immobilization on polymeric surfaces via hydrophobic or dipole-dipole-interactions, to a RGD peptide was investigated. For this purpose, a stearate or an oligo(ethylene glycol) (OEG) was attached to GRGDS in 51–70% yield. The obtained RGD-linker constructs were characterized by NMR, IR and MALDI-ToF mass spectrometry, revealing that the commercially available OEG and stearate linkers are in fact mixtures of similar compounds. The RGD-linker constructs were co-electrospun with poly(*p*-dioxanone) (PPDO). After electrospinning, nitrogen could be detected on the surface of the PPDO fibers by X-ray photoelectron spectroscopy. The nitrogen content exceeded the calculated value for the homogeneous material mixture suggesting a pronounced presentation of the peptide on the fiber surface. Increasing amounts of RGD-linker constructs in the electrospinning solution did not lead to a detection of an increased amount of peptide on the scaffold surface, suggesting inhomogeneous distribution of the peptide on the PPDO fiber surface. Human adipose-derived stem cells cultured on the patches showed similar viability as when cultured on PPDO containing pristine RGD. The fully characterized RGD-linker constructs could serve as valuable tools for the further development of tissue-integrating polymeric scaffolds.

Introduction

Electrospinning of polymers has evolved into a versatile technology for the production of micro- and nanofibrous scaffolds[1, 2] with porous morphologies closely resembling the architecture of the extracellular matrix (ECM).[3] Such non-woven three-dimensional fiber meshes can serve as a substrate for cell seeding.[4] The adhesion of cells on synthetic polymers and their integration in tissues can be promoted by moieties, which can undergo physical interaction with receptor proteins. A prominent example for such a ligand is adhesion

sequences of amino acids such as the tripeptide RGD.[5] Aliphatic polyesters, which are widely applied in temporary implants, lack functional groups allowing covalent coupling of peptides. An interesting option to realize RGD presentation on a polymer fiber is its physical incorporation by co-electrospinning.[6] Leaking of RGD as soluble RGD may, however, inhibit cell adhesion and might promote apoptosis.[7]

Here, the attachment of physical anchor groups to RGD, which enhance the physical interaction to the polymer matrix, and the potential of co-electrospun PPDO/RGD linker construct scaffolds as substrates for cell seeding were explored. Two kinds of anchor groups envisioned to promote the display of hydrophilic peptides on (hydrophobic) polymer matrices in aqueous environments were selected: an oligo(ethylene glycol) (OEG_7) derivative because of its structural similarity to PPDO allowing hydrophic and dipole-dipole interactions and stearate because of its pronounced hydrophobicity. The covalent coupling of such anchor groups to the pentapeptide GRGDS as well as characterization of the synthesized RGD-linker constructs with ^{1}H and ^{13}C NMR, ATR-FTIR and MALDI ToF mass spectrometry is presented. In a subsequent step, these RGD-linker constructs were co-electrospun with PPDO and the presence of the peptides on the surface was assessed by FT-IR and X-ray photoelectron spectroscopy (XPS). Finally, in a preliminary biological evaluation co-electrospun PPDO/OEG_7-GRGDS was compared to PPDO/RGD as a substrate for the growth of human adipose-derived mesenchymal stroma cells (hADSC).

Experimental

GRGDS (H-Gly-Arg-Gly-Asp-Ser-OH) was purchased from Bachem (Bubendorf, BL, Switzerland), stearic acid *N*-hydroxysuccinimide ester was purchased from Sigma-Aldrich (St. Louis, MO, USA) and MeO-OEG_7-NHS was purchased from Broadpharm (San Diego, CA, USA). Polydioxanone (PPDO; Resomer X206S, inherent viscosity of 1.5–2.2 dl/g [0.1% in HFIP, 30 °C], residual monomer content: max. 0.5%) was acquired in the form of white

granules (Evonik Industries AG, Essen, Germany), and 1,1,1,3,3,3-hexafluoro-2-propanol (HFIP) was obtained from Sigma-Aldrich (Gillingham, UK). All other solvents were purchased from commercial suppliers in analytical grade and were used as received.

NMR spectra were acquired on a DRX 500 Avance spectrometer (Bruker, Rheinstetten, Germany). MALDI-ToF spectra were measured on an Ultraflextreme instrument (Bruker Bremen, Germany). ESI-ToF spectra were measured on an Agilent 6210 ESI-TOF instrument (Agilent Technologies, Santa Clara, CA, USA). ATR-FTIR spectra were recorded on Nicolet 6700 FT-IR (Thermo Fisher Scientific, Waltham, MA, USA) and Spectrum 100 FTIR (Perkin Elmer, Waltham, MA, USA) spectrometers.

Synthesis of OEG_7-GRGDS:

GRGDS (51.6 mg, 105 µmol) and MeO-OEG_7-NHS (53.6 mg, 105 µmol) were dissolved in a mixture of DMSO and H_2O (10:1, 2.8 ml) and were stirred at room temperature for 1 day. The solvent was removed under reduced pressure and the remaining residue was filtered through silica gel (200-400 mesh, 60 Å) with EtOAc/MeOH = 1:1 as eluent. After removal of the solvent under reduced pressure, the obtained crude product was purified by reverse phase HPLC [*Varian Prostar* HPLC system, *Polymer Laboratories* PLRP-S column (1212-6800, 300 × 25 mm, 100 Å pore size, 8 µm particle size), UV detector (υ = 254 and 220 nm)] using a gradient between solution A (90% H_2O, 10% MeCN, 0.1%TFA) and solution B (90% MeCN, 10% H_2O, 0.1% TFA) at a flow rate of 8 ml/min. After lyophilization of the product fractions, MeO-OEG_7-GRGDS was obtained as a colorless oil (47 mg, 51%).

^{1}H NMR (500 MHz, DMSO-d_6): δ = 12.51 (bs, 2H, COOH), 8.26 (t, *J* = 5.7 Hz, 1 H, $NH_{(Gly)}$), 8.17 (d, *J* = 8.0 Hz, 1H, $NH_{(Asp)}$), 8.09 (t, *J* = 5.7 Hz, 1H, $NH_{(Gly)}$), 8.04 (d, *J* = 7.8 Hz, 1H, $NH_{(Arg)}$), 7.90 (d, *J* = 7.9 Hz, 1H, $NH_{(Ser)}$), 7.57 (t, *J* = 5.8 Hz, 1H, $NH_{(Arg)}$), 7.37–6.98 (2 brs, 3H, $NH_{(Arg)}$), 4.68–4.64 (m, 1H, $CH_{(Asp)}$), 4.29 (m, 1H, $CH_{(Arg)}$), 4.23 (m, 1H, $CH_{(Ser)}$), 3.75–3.58, (3 m, 6H, $CH_{2(Gly)}$, $CH_{2(Ser)}$), 3.50 (bs, 28H, OCH_2), 3.44 (m_c, 2H, $CH_3OC\mathit{H}_2$), 3.23

(s, 3H, OCH_3), 3.08 (m, 2H, $CH_{2(Arg)}$), 2.69 (dd, *J* = 16.6, 5.2 Hz, 1H, $CH_{2(Asp)}$), 2.49 (dd, *J* = 16.6, 5.2 Hz, 1H, $CH_{2(Asp)}$), 2.39 (t, *J* = 6.3 Hz, 2H, $OCH_2C\mathit{H}_2CONH$), 1.70, 1.55–1.46 (3 m, 2H, 1H, 1H, $CH_{2(Arg)}$) ppm. The Signal for $OH_{(Ser)}$ could not unambiguously be assigned. **^{13}C NMR** (126 MHz, DMSO-d_6): δ = 171.74, 171.70*, 170.65, 170.63, 169.1, 168.6, 169.2, 168.4 (6 s, CO), 156.8 (s, $NHCNH_2$), 71.3 (t, CH_3OCH_2), 69.8**, 69.7, 69.6, 66.5 (4 t, OCH_2), 61.3 (t, $CH_{2(Ser)}$), 58.1 (q, OCH_3), 54.8 (d, $CH_{(Ser)}$), 52.2 (d, $CH_{(Arg)}$), 49.2 (d, $CH_{(Asp)}$), 42.0, 41.9 (2 t, $CH_{2(Gly)}$), 40.4 (t, $CH_{2(Arg)}$), 36.3 (t, $CH_{2(Asp)}$), 35.9 (t, OCH_2CH_2CONH), 29.1, 24.9, (2 t, $CH_{2(Arg)}$) ppm. *Signal with high intensity corresponds to two carbon atoms. **Signal with very high intensity, corresponds to multiple carbon atoms of the OEG chain. **IR** (ATR): ν = 3300–3200 (N—H, O—H), 3065, 2920–2875 (C—H), 1650, 1530 (C=O), 1195, 1120–1095, 1025, 1005 cm^{-1}. **MS** (MALDI): $[M + H]^+$: $C_{35}H_{65}N_8O_{18}^+$ calcd.: 885.44 m/z; found: 885.89 m/z, $[M + Na]^+$ $C_{35}H_{64}N_8NaO_{18}^+$ calcd.: 907.42 m/z; found: 907.80 m/z. **MS** (ESI-TOF): $[M + H]^+$: $C_{35}H_{65}N_8O_{18}^+$ calcd.:885.4411 m/z; found: 885.4421 m/z; $[M + Na]^+$: $C_{35}H_{64}N_8NaO_{18}^+$ calcd.: 907.4231 m/z; found: 907.4259 m/z.

Synthesis of Stearate-GRGDS:

GRGDS (25.2 mg, 51.4 μmol) and stearic acid *N*-hydroxysuccinimide ester (19.6 mg, 51.4 μmol) were suspended in a mixture of CH_2Cl_2, DMSO and H_2O (1:1.4:1, 6.5 ml) and were vigorously stirred at room temperature for 14 days. The solvent was carefully removed under reduced pressure. The obtained residue was treated with MeOH/EtOAc (1:1, 3 ml) to give a colorless precipitate that was collected by centrifugation. The obtained crude product was washed with EtOAc/MeOH (9:1, 10 ml), EtOAc/CH_2Cl_2 (5:1, 8 ml) and EtOAc (6 ml). Drying under reduced pressure provided stearate-GRGDS as a colorless solid (27.0 mg, 69%). The MS spectra show additional signals [M-28] indicating that the product also contains the corresponding palmitate GRGDS derivate.

^{1}H NMR (500 MHz, DMSO-d_6): δ = 10.00 (bs, 2H, COOH), 8.60–8.57, 8.18, 7.34, 7.10 (m, 3 s, 3H, 2H, 1H, 3H, NH), 4.38–4.34 (m, 1H, NCH_{Asp}), 4.27–4.23 (m, 1H, $NCH_{(Arg)}$), 3.88 (dd, *J* = 11.8, 6.0 Hz, 1H, $NCH_{(Ser)}$), 3.72, 3.71 (2 s, 2H each, $CH_{2(Gly)}$), 3.58–3.51 (m, 2H, $CH_{2(Ser)}$), 3.19–3.10, 3.00–2.97 (2 m, 1H each, $CH_{2(Arg)}$), 2.36–2.32, 2.62–2.55 (2 m, 1H each, $CH_{2(Asp)}$), 2.14–2.06 (m, 2H, CH_2CH_2CO), 1.97–1.86, 1.70–1.59, 1.57–1.49, (3 m, 2H, 1H, 1H, $CH_{2(Arg)}$), 1.49–1.40 (m, 2H, CH_2CH_2CO), 1.23 (s, 28H, CH_2), 0.85 (t, *J* = 6.8 Hz, 3H, CH_3) ppm. The signal for $OH_{(Ser)}$ could not unambiguously be assigned. **^{13}C NMR** (126 MHz, DMSO-d_6): δ = 174.8, 172.7, 172.5, 170.5, 169.3, 168.6, 164.3, (7 s, C=O), 157.3 (s, C=NH), 62.3 (t, $CH_{2(Ser)}$), 55.4 (d, $CH_{(Ser)}$), 52.4 (d, $CH_{(Arg)}$), 49.9 (d, $CH_{(Asp)}$), 42.6, 42.0 (2 t, $CH_{2(Gly)}$), 40.6 (t, $CH_{2(Arg)}$), 37.5* (t, $CH_{2(Asp)}$), 35.2 (t, C-2), 32.1 (t, C-17), 31.3 (t, $CH_{2(Arg)}$), 29.07, 29.02, 28.97, 28.9, 28.7 (5 t, CH_2), 25.2 (t, C-3), 24.5 (t, $CH_{2(Arg)}$), 22.1 (t, CH_2), 14.0 (q, C-18) ppm. **IR** (ATR): ν = 3415–3070 (N—H, O—H), 2925, 2845 (C—H), 1640, 1530 (C=O), 1460, 1385, 1235 cm^{-1}. **MS** (MALDI): $[M + H]^+$: $C_{35}H_{65}N_8O_{10}^+$ calcd.: 757.48 m/z; found: 757.00 m/z; $[M' + H]^+$: $C_{33}H_{61}N_8O_{10}^+$ calcd.:729.45 m/z; found: 729.53 m/z. **MS** (ESI-TOF): $[M + H]^+$: $C_{35}H_{65}N_8O_{10}^+$ calcd.: 757.4818 m/z; found: 757.4814 m/z; $[M + Na]^+$: $C_{35}H_{64}N_8O_{10}Na^+$ calcd.: 779.4638 m/z; found: 779.4630 m/z; $[M' + H]^+$: $C_{33}H_{61}N_8O_{10}^+$ calcd.: 729.4504 m/z; found: 729.4504; $[M' + Na]^+$: $C_{33}H_{60}N_8O_{10}Na^+$ calcd.: 751.4325 m/z; found: 751.4318 m/z.

Electrospinning:

PPDO (9% w/v in HFIP) solutions with two different concentrations of MeO-OEG_7-GRGDS or stearate-GRGDS were prepared by dissolving 0.18 g of PPDO in 2 ml of HFIP. Either 0.5 mg/ml or 1.4 mg/ml of the RGD constructs was added. The mixture was stirred for 3 h at room temperature to achieve complete dissolution of the polymer and the respective RGD construct. The solutions were electrospun in a custom built electrospinning setup (Supporting Information Fig. S1). The solutions were dispensed through a 20G stainless steel needle

(ID ~600 µm) (Precision Tips, Nordson EFD, Ohio, USA) from a 10 ml polypropylene syringe mounted on a syringe pump (Cole-Palmer infusion pump EW-74900-05, Cole-Parmer, London, UK) at a flow rate of 1 ml/h for all four solutions. The needle was connected to a high-voltage DC power supply (HCP35-35000, FuG Elektronik, Rosenheim, Germany). Aluminum foil was placed on top of the grounded collector that was used to collect the fibers. The distance from the needle to the collector was 12 cm. The electrospinning was carried out at room temperature and relative humidity of 25 ± 3 °C and 33 ± 8%, respectively.

PPDO patches co-electrospun with unmodified (free) RGD (Ac-Gly-Arg-Cys-Gly-Arg-Gly-Asp-Ser-Pro-Gly-NH_2) were prepared as previously reported.[6]

Electron microscopy:

The morphological properties of the samples were characterized using scanning electron microscopy (SEM; Quanta 200 FEG ESEM instrument, FEI, Hillsborough, OR, USA). Samples were sputtered with a gold coating (10 nm thickness) prior to SEM analysis. The images obtained were then analyzed using the ImageJ software, and the fiber diameters (based on > 50 measurements) were calculated. The jPOR plugin for ImageJ was additionally used to determine the porosity of the samples. In order to improve the reliability of the calculation, at least five SEM images were used to calculate the porosity for each sample.

X-ray photoelectron spectroscopy (XPS):

Surface composition was determined by XPS on a K-Alpha XPS (Thermo Scientific, East Grinstead, UK). The X-ray source was a microfocused monochromatic Al-Kα with an energy of 1486.6 eV. Typically, three positions per sample were analyzed, with a spot size of 400 × 800 µm, and an emission angle of 0°.

Biological Evaluation:

Human ADSCs were isolated from subcutaneous fat obtained from patients undergoing liposuction at Saint-Louis Hospital, Paris, France with informed consent (Ethics committee approval No.: 2010-07-10). Briefly, adipose tissue was washed in prewarmed sterile PBS, after which the tissue was enzymatically dissociated through incubation for 45 min at 37 °C with collagenase NB6 (SERVA Eletrophoresis). After digestion, filtration on 100 µm filters and numeration, cells were resuspended in alphaMEM (Macopharma) supplemented with 10% fetal bovine serum (FBS) and 1% of antibiotic-antimycotic solution. Then, cells were seeded at 10,000 cells/cm². Medium was changed twice a week, and at confluence cells were dissociated with trypsin (Hyclone). hADSC phenotype was analyzed by flow cytometry. The following monoclonal antibodies were used: CD29-FITC (Beckman Coulter), CD44-FITC (BD Pharmingen), CD73-PE (BD Pharmingen), CD90-FITC (BD Pharmingen), CD105-PE (R&D System), CD31-FITC (BD Pharmingen), CD34-FITC (Beckman Coulter) and CD45-FITC (BD Pharmingen). Isotype control antibodies were included in all experiments: MsIgG1 isotype-FITC (BD Pharmingen) and MsIgG2b isotype-PE (Miltenyi biotec). Isolated hADSC were seeded on 1 cm² patches, preliminary sterilized in 70% ethanol, at three densities for two days. Cell viability on the seeded grafts was assessed by an MTT (3-[4, 5-dimethylthiazolyl-2]-2, 5-diphenyltetrazolium bromide) assay. Briefly, 1 cm^2 patches were seeded with 10^5, 10^6 or 3.5×10^6 hADSCs for 48 h. Subsequently 10 µl of 5 mg/ml MTT solution (Sigma-Aldrich) for 100 µl medium was added in each well. After 2 h of incubation at 37 °C, each sample was transferred in a 96-well plate and read with an ELISA plate reader (test wavelength of 570 nm, reference wavelength of 630 nm).

Results and Discussion

For this study, two chemically different moieties were selected to be attached to the peptide GRGDS to serve as anchor groups for enhanced adhesion on a PPDO matrix, an OEG_7 and a

stearate. Stearate is more hydrophobic and may potentially allow stronger hydrophobic interactions with the polymer matrix. OEG_7 with its ether repetition unit is structurally more similar to PPDO and may allow hydrophobic as well as dipole-dipole interactions resulting in co-localization with the polymer during the electrospinning. The more hydrophilic peptide part might then be displayed on the surface when an orientation of the RGD-linker constructs during the electrospinning and evaporation occurs, which may be supported by the higher steric demand of the peptide part. OEG_7 and stearate are commercially available as NHS-activated monofunctionalized species, and both have a similar molar mass—267 $g \cdot mol^{-1}$ for the stearate moiety and 395 $g \cdot mol^{-1}$ for the OEG_7—slightly lower than that of the RGD peptide with 490 $g \cdot mol^{-1}$. For the targeted application, to promote a more efficient tissue integration of polymer scaffolds, the anchor moieties should feature sufficient size (molecular weight) to allow efficient physical interactions with the polymer matrix while being small enough with respect to the size of the RGD-peptide. In this way, its biointeractions and therefore biological activity are not reduced.

Attachment of GRGDS to the anchor groups was realized by reaction of the *N*-terminus of GRGDS with the *N*-hydroxysuccinimidylated linkers in solution at room temperature (Figure 1). In case of the stearate linker, a biphasic solvent mixture and vigorous stirring were employed, as no solvent capable of dissolving both the hydrophobic stearate NHS ester and the hydrophilic peptide could be identified. The reaction process was followed by consumption of the peptide via ninhydrin staining on silica TLC plates.

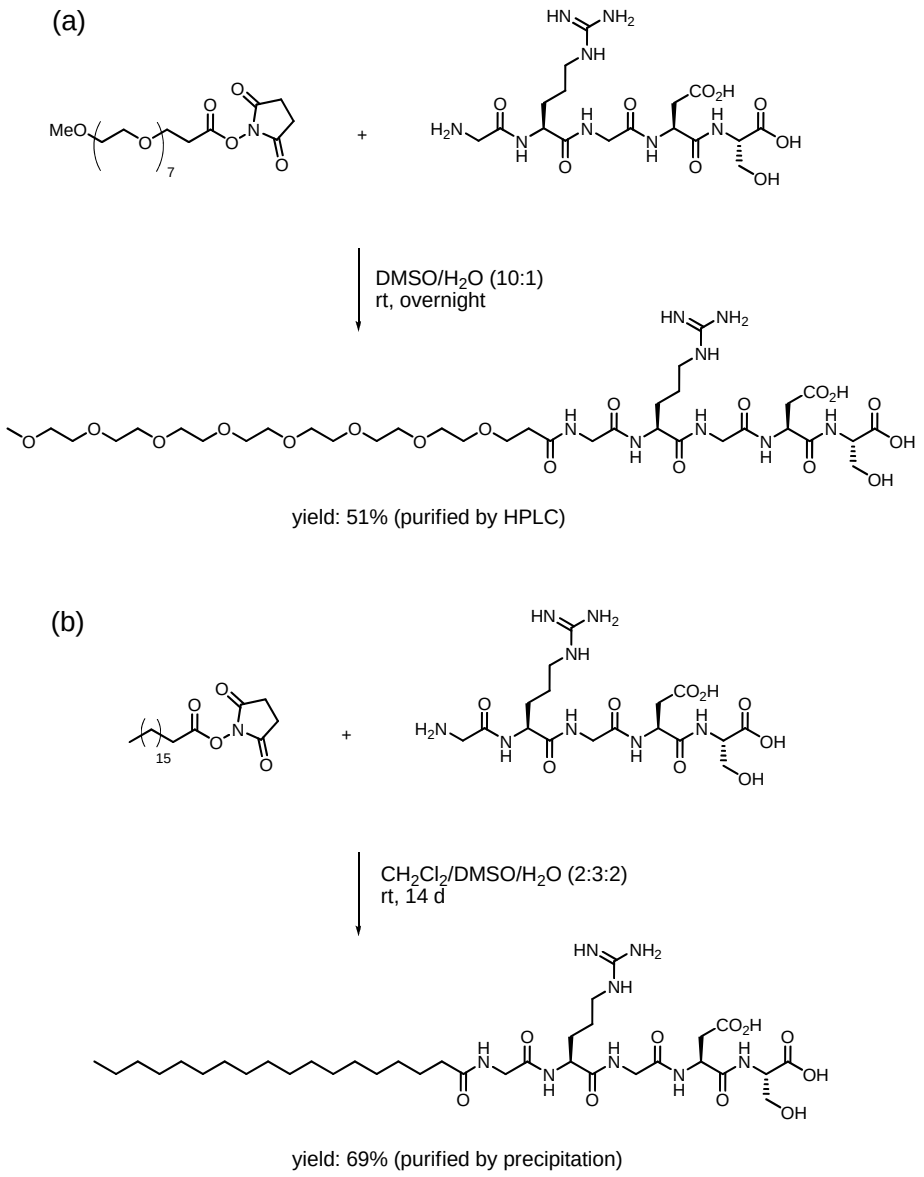

Figure 1. (a) Coupling of GRGDS to OEG_7-NHS ester; (b) coupling of GRDGS to stearic acid NHS ester.

While the stearate adduct could be isolated by precipitation in 69% yield, the OEG_7 adduct required HPLC purification, resulting in a slightly lower yield (51%). The products were characterized by ^{1}H- and ^{13}C NMR as well as FT-IR spectroscopy and mass spectrometry. In the NMR and IR spectra (see Supporting Information Figs S2 and S3), signals of both components were found, and integration of the ^{1}H-NMR signals showed the correct ratio of the two components (1:1 coupling) and no presence of unreacted starting materials. However, more detailed analysis by MALDI-ToF (Figure 2) and ESI mass spectrometry revealed that in

both cases the linker starting materials were not pure, but contained structurally related derivatives. This contamination led into formation of corresponding GRGDS by-products in the coupling step that were not efficiently removed by the employed purification methods.

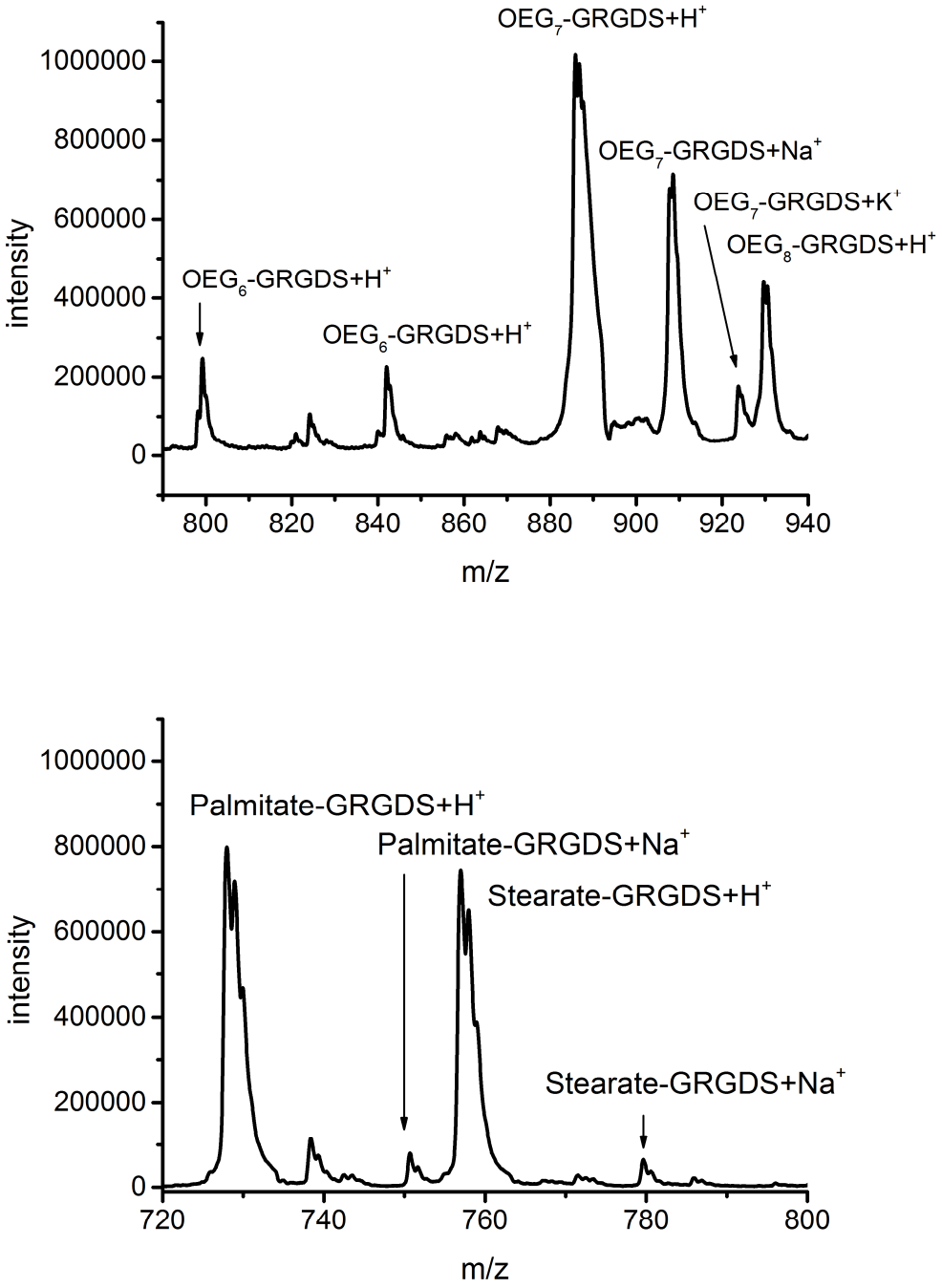

Figure 2. Excerpts of the MALDI ToF spectra of OEG_7-GRGDS (top) and stearate-GRGDS (bottom) showing expected signals for the desired coupling products and in addition signals for structurally related by-products.

In the case of the OEG anchor group, not only the OEG_7 species, but also OEG_6, OEG_8, and, to a minor extent, also OEG of other lengths were present in the samples and could not be completely separated from OEG_7 by HPLC. Given the synthetic routes used, such impurities are generally anticipated in oligomers; interestingly, the stearate also contained impurities of a similar compound, in this case the corresponding palmitate. While in view of the planned use in the co-electrospinning, the identified impurities did not interfere, it is important to note that a detailed analysis of compounds is recommended in such syntheses, as without the mass spectrometry the presence of mixtures would not have been disclosed.

In a next step, mixtures of the RGD linker constructs in two different ratios (1.4 or 0.5 mg/ml, corresponding to 1.5 or 0.5 wt% content) and PPDO were co-electrospun (electrospinning setup: see Supporting Information Fig. S1). Figure 3 depicts electron microscopy pictures of the electrospun non-woven mats. In all cases, the co-electrospinning proceeded well, and the fiber orientation, fiber diameter, and porosity (see Table 1) were comparable for all investigated samples and are very similar to pure electrospun PPDO.[6]

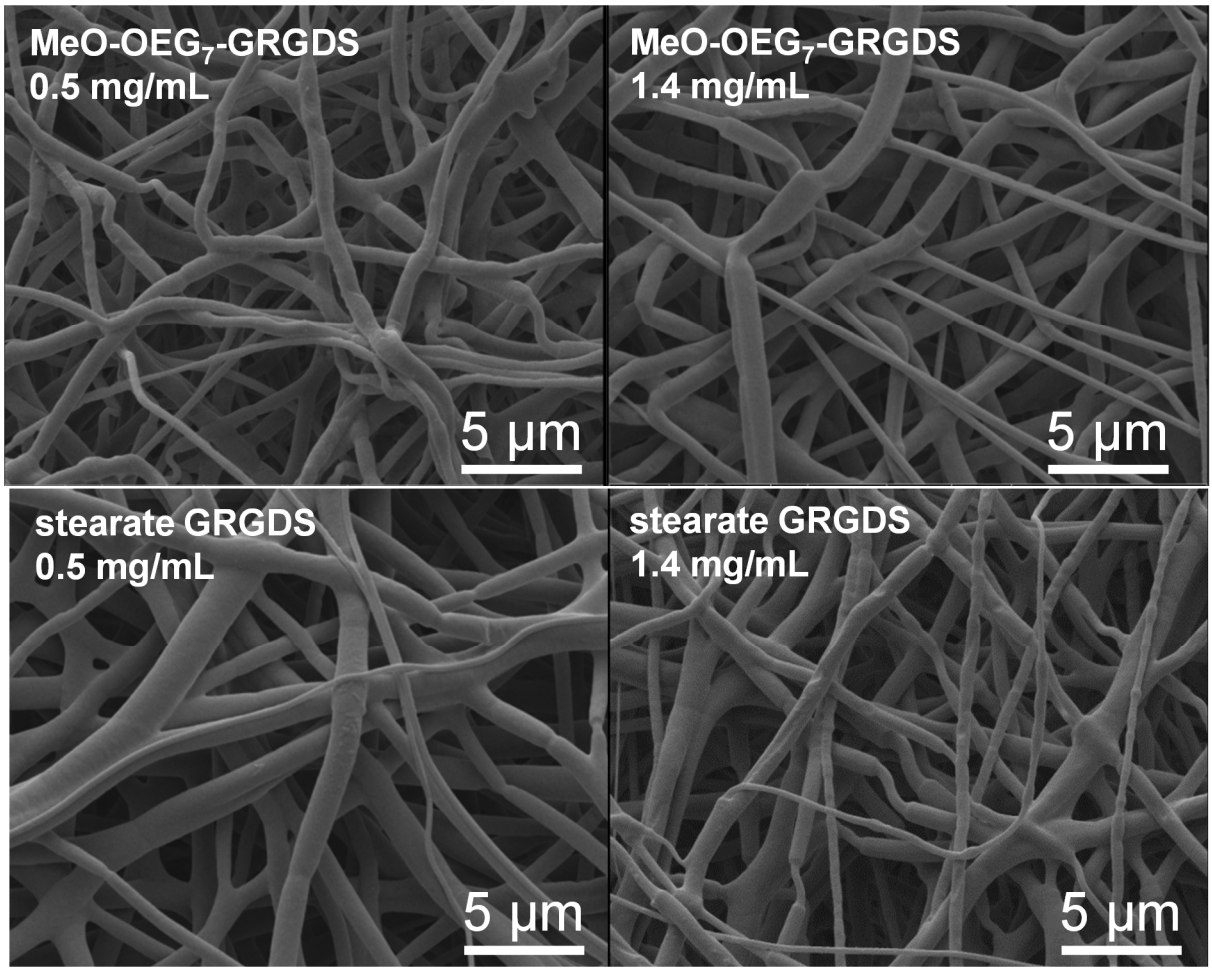

Figure 3. Electron microscopy pictures of fibers co-electrospun from solutions of PPDO with OEG_7-GRDGS (top) or stearate-GRGDS (bottom). The concentration of RGD-linker constructs did not significantly influence the fiber diameters.

Table 1. Fiber diameters and porosities of the co-electrospun PPDO patches.

Co-electrospinning additive	Fiber diameter ± standard deviation [nm]	Porosity ± standard deviation [%]
OEG_7-GRGDS 0.5 mg/ml	894 ± 57	47 ± 1
OEG_7-GRGDS 1.4 mg/ml	832 ± 44	48 ± 0.5
Stearate-GRGDS 0.5 mg/ml	803 ± 44	45 ± 0.5
Stearate-GRGDS 1.4 mg/ml	903 ± 48	44 ± 0.2

It was expected that by increasing the amount of GRGDS linker constructs in solution, the peptide content in the fibers would also increase. This was investigated by FT-IR and XPS. The FT-IR spectra (Supporting Information Fig. S4) showed only absorptions indicative of

PPDO, while the peptide could not be detected. This is likely to be related to the low content of peptide in the overall matrix (≤2 wt%).

In the XPS, the presence of the peptide on the surface could be demonstrated by the occurrence of a nitrogen signal, which was not present in the pure PPDO sample (Table 2). It should be noted that for a homogeneous distribution of the peptide in the matrix, the expected nitrogen content would be lower (0.2–0.5 at%) than found (0.5–1.4 at%). This suggests a preferential presentation of the peptide on the surface of the fibers rather than its embedding into the PPDO matrix.

Table 2. Surface composition of PPDO co-electrospun with RGD-linker constructs in different compositions and pure PPDO, determined by XPS.

RGD type and conc. (mg/ml)	Surface C (at.%)	Surface N (at.%)	Surface O (at.%)
OEG_7 0.5 mg/ml	66.2 ± 1.5	0.9 ± 0.1	33.0 ± 1.4
OEG_7 1.4 mg/ml	64.0 ± 1.9	0.5 ± 0.1	35.5 ± 2.0
Stearate 0.5 mg/ml	65.7 ± 0.8	1.4 ± 0.1	33.0 ± 0.9
Stearate 1.4 mg/ml	67.9 ± 0.7	0.7 ± 0.2	31.4 ± 0.7
PPDO	58.1 ± 0.4	0.0	38.7 ± 0.2

The stearate compound was associated with a somewhat higher nitrogen presence on the surface, which may indicate an orientation of the RGD-linker-construct with the more hydrophobic part being embedded in the polymer matrix, while the peptide part is on the surface. In case of the OEG linker, this orientation is presumably less pronounced. Interestingly, the nitrogen content did not increase with the concentration of the linker construct. What should be furthermore considered is the rather limited surface area, which can be analyzed by XPS, so it is also conceivable that the peptide is not homogeneously distributed on the surface, but that microphase separation phenomena in the solution used for electrospinning have resulted in an inhomogeneous display of the peptide. In a previous study, co-electrospun PPDO/RGD-peptide without physical anchor groups[6] showed slightly higher

nitrogen content (peptide concentration) at the fiber surface measured by XPS. This may indicate a higher embedding extent of the RGD-linker constructs into the PPDO matrix than in the case of non-functionalized RGD. This could potentially translate into a prolonged presentation of the biologically active peptide on the polymer matrix surface over time during the course of hydrolytic degradation of the polymer matrix in vivo.

In a preliminary biological evaluation, hADSC were cultured on the patches containing OEG_7-GRGDS, and cell viability was determined by a MTT assay. This colorimetric test measures the chemical reduction of MTT into formazan, which is directly proportional to the number of viable cells. The results were compared to hADSC cultured on PPDO co-electrospun with a pristine RGD peptide (Figure 4). While the number of viable cells expectedly increased with increased initial cell densities, viability was actually not significantly different for the different types of RGD peptide (pristine or linker-bound) and was comparable to pure electrospun PPDO.[6]

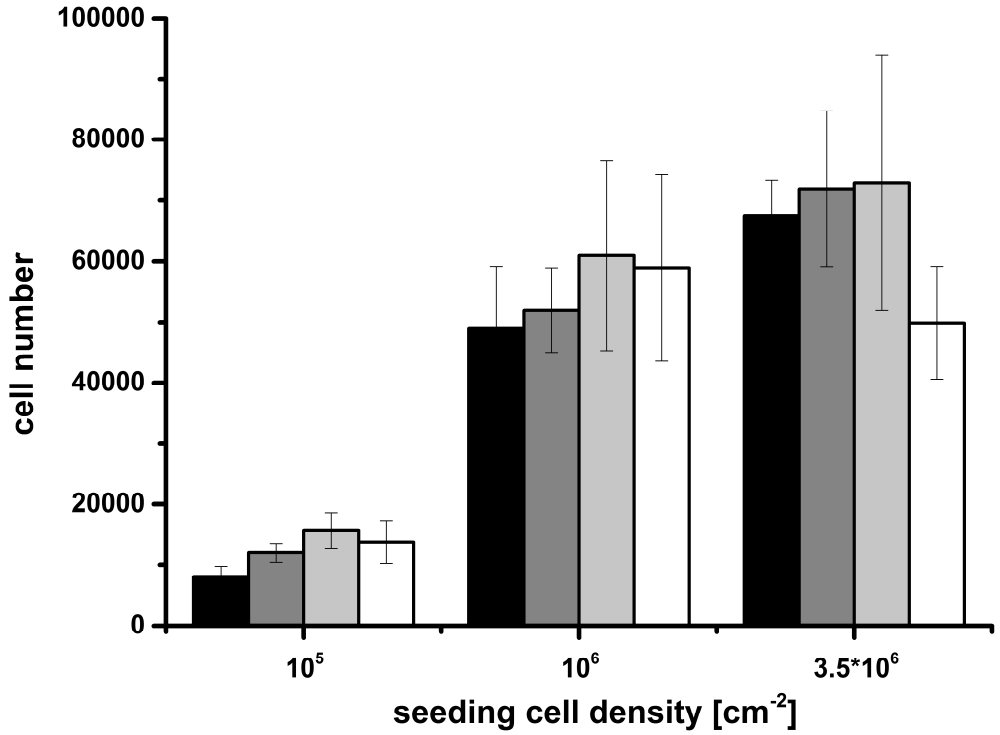

Figure 4. Viability of human adipose-derived stem cells (MTT-test) cultured on electrospun patches of PPDO containing non-functionalized RGD peptide and RGD linker construct in different concentrations; co-electrospinning additives from left to right: non-functionalized RGD (0.5 (■) and 1.4 (■) mg/ml) and OEG_7-GRGDS (0.5(■)/1.4 (□) mg/ml).

Conclusion

RGD constructs with physical anchor groups were successfully synthesized and could be co-electrospun with PPDO into nanofibers, putatively with hydrophobic interactions stabilizing the construct within the core of the matrix while the hydrophilic peptide is preferentially presented on the surface. Incorporation of RGD did not affect the fiber morphology of the electrospun scaffolds. RGD could be detected on the surface by XPS, but not by IR. The increase in RGD in the feeding solution did not lead to increased RGD display, suggesting that either the RGD is partially embedded into the fibers and/or that its distribution is inhomogeneous. In any case, the fully characterized RGD-linker constructs add to the toolbox of biomaterial scientists for the further development of tissue integrating polymers as they

offer the possibility for an enhanced adhesion of the biological active moiety (RGD-peptide) through physical interactions at the interface between the polymer matrix and living tissue. While the present report is focused on the synthesis of the RGD linker-constructs and its utilization for co-electrospinning, additional studies to compare the tissue integration of co-electrospun PPDO/RGD-linker constructs to that of PPDO/non-functionalized RGD scaffolds are required to fully explore the potential of the presented linker constructs in vivo.

Acknowledgements

This project has received funding from the European Union's Seventh Framework Programme for research, technological development and demonstration under grant agreement no 604049. X-ray photoelectron spectra were obtained at the National EPSRC XPS Users' Service (NEXUS) at Newcastle University, an EPSRC Mid-Range Facility.

References

[1] T. J. Sill, H. A. von Recum, *Biomaterials* **2008**, 29, 1989.
[2] W. Cui, Y. Zhou, J. Chang, *Sci. Technol. Adv. Mater.* **2010**, 11, 014108.
[3] C. Vaz, S. Van Tuijl, C. Bouten, F. Baaijens, *Acta Biomater.* **2005**, 1, 575.
[4] T. S. Karande, J. L. Ong, C. M. Agrawal, *Ann. Biomed. Eng.* **2004**, 32, 1728.
[5] U. Hersel, C. Dahmen, H. Kessler, *Biomaterials* **2003**, 24, 4385.
[6] M. Pontailler, E. Illangakoon, G. R. Williams, C. Marijon, V. Bellamy, D. Balvay, G. Autret, V. Vanneaux, J. Larghero, V. Planat-Benard, M.-C. Perier, P. Bruneval, P. Menasché, D. Kalfa, *Tissue Eng., Part A* **2015**, 21, 1552.
[7] C. D. Buckley, D. Pilling, N. V. Henriquez, G. Parsonage, K. Threlfall, D. Scheel-Toellner, D. L. Simmons, A. N. Akbar, J. M. Lord, M. Salmon, *Nature* **1999**, 397, 534.